INDIAN JOURNAL OF SCIENCE AND TECHNOLOGY

RESEARCH ARTICLE

Check for updates

OPEN ACCESS

Received: 08-11-2023

Accepted: 07-01-2024

Published: 20-02-2024

Study of Active Medium Length Effect on Characteristics of Passive Q-Switching and Stokes with Anti-Stokes Pulse

Dunya Saad Hussein[1]*, Abdul-Kareem Mahdi Salih[1]

1 Physics Department, College of Science, Thi-Qar University, Thi-Qar, Iraq

Citation: Hussein DS, Salih AKM (2024) Study of Active Medium Length Effect on Characteristics of Passive Q- Switching and Stokes with Anti-Stokes Pulse. Indian Journal of Science and Technology 17(8): 723-731. https://doi.org/10.17485/IJST/v17i8.2823

* **Corresponding author**.

matrix199408@gmail.com

Funding: None

Competing Interests: None

Published By Indian Society for Education and Environment (iSee)

ISSN
Print: 0974-6846
Electronic: 0974-5645

Abstract

Objective: To study the effect of active medium length on the characteristics of passive Q-switching pulses, Stokes pulses, and anti-Stokes pulses generated by laser-Raman medium interaction in optical systems, theoretically. **Methods:** The optical system consists of Nd^{+3}:YVO_4, $PbWO_4$, and Cr^{+4}:YAG as active mediums, Raman medium, and saturable absorber materials, respectively. The rate equations model has been used in the study, and the Rung-Kutta-Fehelberg numerical method was used to solve the rate equations. **Finding:** The result shows that, decreasing of the active medium length leads to emit high power pulses at advanced time. It also leads to increase in initial value and the maximum value of population inversion density, and leads to increase in the energy of passive Q-switching pulses, Stokes pulses, and anti-Stokes pulses. So the decreasing of the active medium length leads to decrease in the pulses duration and the final population inversion density. To increase the power of the three generated pulses, the length of the active medium used in the system must be decreased. **Novelty:** The characteristics of two pulses generated by Laser-Raman interaction (passive Q-switching pulse and Stokes pulse) have been of interest in some studies. This study investigates the effect of the active medium length on the characteristics of three pulses generated (anti-Stokes pulse with Stokes pulse as well as the passive Q-switching pulses) by the optical system rather than two pulses.

Keywords: Laser; Nd^{+3} :YVO_4; passive Q-switching pulse; Stokes and anti--Stokes pulses 1

1 Introduction

Q-switching is a preferred technique for generating short pulses with high peak power. The pulses generated from Q-switching are typically produced at low repetition rates in the kHz range [1,2]. Organic dyes, doped crystals, and semiconductors are common materials used in passive Q-switches (PQS) [3]. PQS is the method using a saturable absorber (SA) [4]. SA based on Cr^{+4} has been known and used for many years. Crystal-based Cr^{+4}: YAG has been widely employed in passive Q-switching techniques, although they share all of the limitations of single crystal technology, such as long manufacturing times, poor compatibility for large and composite structures, and so on [5]. Cr^{4+}:YAG crystal has a wide absorption band at 0.9–1.2μm when compared with other SA [3]. The energy level diagram of Cr^{+4}:YAG shown in Figure 1 [6]. Ions are excited from ground level 1 to an intermediate level 3 after the absorption of a pumping photons; from here, non-radiative relaxation to the first excited level (level 2) occurs. The ions either relax to the ground level with a life time of level 2 or promoted to the higher excited level (level 4) by the absorption of another photon. Relaxation to the first excited level 2 is again non-radiative with a lifetime, the ions in the higher excited level 4 quickly relax back to the initial excited level 2 due to the lifetime of the higher excited level is much shorter than the pulse duration [6].

Nd^{+3}:YVO_4 is a well-active medium (AM) that is mainly used in Q-switched laser systems. With the latest technology, it displays short laser pulses with duration comparable to one round-trip and switchable operation between 1064 nm Q-switched pulses [7]. The Nd^{+3}:YVO_4 crystals have a large cross-section of excited radiation, and they are typically used in low- or medium-power lasers because of their limited thermal conductivity [8]. Nd^{+3} ion has many permissible transitions from the metastable level $^4F_{3/2}$ to the lower lying energy Stark sublevels $^4I_{13/2}$, $^4I_{11/2}$, and $^4I_{9/2}$, respectively, resulting in possible laser radiations at 1.3, 1.06, and 0.9μ m. Pump bands are placed above the top laser level, beginning with the manifold $^4F_{5/2}$, which is responsible for absorption around 800 nm. The greatest emission cross-sections in Nd^{+3} doped laser material for $^4F_{3/2} \rightarrow ^4I_{11/2}$ transitions emitting radiation at 1.06μm are shown in Figure 2 [9].

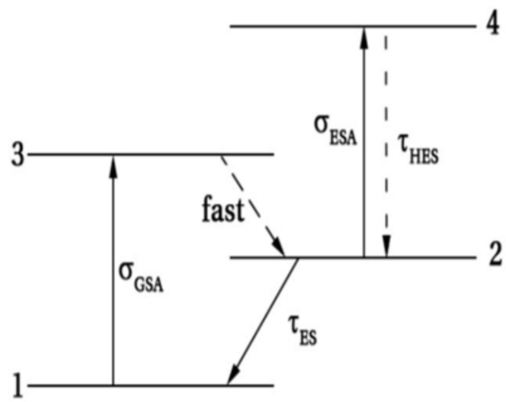

Fig 1. Schematic representation of the energy levels of Cr^{+4}:YAG [6]

Stimulated Raman scattering (SRS) is a way that shifts the existing wavelength to a new one (also known as Raman shift). When the pump and Stokes photons are applied simultaneously, the new generator has a stable output wavelength, thin line width, and fantastic directionality, which is substantially improved when a specific quantity of pump photons are transformed into Stokes photons [10]. The structural tunglevels $CaWO_4$, $SrWO_4$, $BaWO_4$, and Lead tunglevel ($PbWO_4$) are compounds which have properties and their multiple. These materials can grow as single crystals [11]. $PbWO_4$ is a popular scintillator for high-energy physics, known for its low cost, easy growth, broad transmittance spectrum, high optical damage threshold, and strong gain coefficient, with many remaining Raman crystals created. $PbWO_4$ occurs naturally in two forms: stolzite (scheelite structure with WO_4 tetrahedra) and Raspite (overlapping WO_6 octahedra), with the latter being synthesized. [12,13]

This study investigates the effect of the active medium length on characteristic of three pulses generated by the optical system. These pulses are anti-Stokes pulse with Stokes pulse as well as the passive Q-switching pulse.

2 Methodology

A mathematical rate equations model [14], as shown in the Equations (1), (2), (3), (4), (5) and (6) has been used to study the effect of active medium length on the characteristic of PQS, Stokes, and anti-Stokes pulses where generates by optical system.

$$\frac{d\varnothing_L}{dt} = \varnothing_L \left[k_g N_g - k_a N_{ag} - \beta k_a N_{ae} - \frac{2ghcv_s \varnothing_s l_R}{\tau_{Rt}} - \frac{2ghcv_{as} \varnothing_{as} l_R}{\tau_{Rt}} - \frac{1}{\tau_L} \right] \quad (1)$$

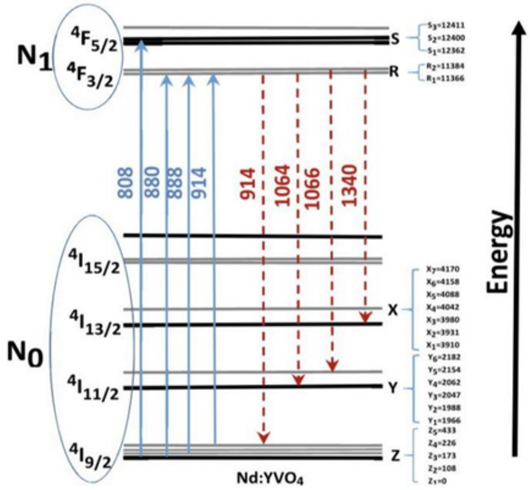

Fig 2. Schematic representation of the energy levels of Nd^{+3}:YVO_4 [9]

$$\frac{d\varnothing_S}{dt} = \varnothing_S\left[\frac{2ghcv_s\varnothing_L l_R}{\tau_{Rt}} - \; k_a N_{ag} - \beta k_a N_{ae} - \frac{1}{\tau_S}\right] + K_{SP}\varnothing_L \tag{2}$$

$$\frac{d\varnothing_{as}}{dt} = \varnothing_{as}\left[\frac{2ghcv_{as}\varnothing_L l_R}{\tau_{Rt}} - \; k_a N_{ag} - \beta k_a N_{ae} - \frac{1}{\tau_{as}}\right] + K_{SP}\varnothing_L \tag{3}$$

$$\frac{dN_g}{dt} = R_p - \gamma_g N_g - \gamma_p k_g N_g \varnothing_L \tag{4}$$

$$\frac{dN_{ag}}{dt} = -K_a N_{ag}\varnothing_L - k_a N_{ag}\varnothing_s - k_a N_{ag}\varnothing_{as} + \gamma_a N_{ae} \tag{5}$$

$$\frac{dN_{ae}}{dt} = K_a N_{ag}\varnothing_L + K_a N_{ag}\varnothing_s + k_a N_{ag}\varnothing_{as} - \gamma_a N_{ae} - \beta K_a N_{ae}\left(\varnothing_s + \varnothing_{as}\right) \tag{6}$$

The physical meaning of the six equations above is explained as following:

Equations (1), (2) and (3) describes the time variation of laser photons density, Stokes photons density and anti-Stokes photons density respectively, Equation (4) describes the population inversion density (PID) and Equations (5) and (6) describes the time variation of population of SA ground and excite level receptivity. Before we explain the terms of these equations, it is necessary to point out that the terms in positive sign considered the source of additives in each equation, while the terms in negative sign considered the source of decrease in each equation.

The terms of Equation (1) can be defined as the following, the first term represents the laser photons density which are emitted by the stimulated emission, the second and the third term is the number density of laser photons which absorbed by the ground and excited state of SA respectively. The fourth and the fifth term represent the laser photons lost due to the generation of the photons Stokes and anti- Stokes in Raman medium, the sixth term represents the losses resulting from the cavity decay due to the absorption, scattering, reflection of photons in different directions without return to the AM. The terms of Equation (2) can be defined as the following, the first term is the Stokes photons which are emitting from RM, the second and the third term represent the absorption of Stokes photons in the ground and excited levels of SA, the fourth term represents the losses of Stokes photons due to cavity decay (absorption, scattering, reflection of photons in different directions without return to the RM), the fifth term represents all the Stokes photons resulting from the spontaneous scattering in Raman medium.

While the terms of Equation (3) can be defined as the following, the first term is the anti-Stokes photons which are emitting from RM, the second and the third term represent the absorption of anti- Stokes photons in the ground and excited levels of SA, the fourth term represents the losses of ant-Stokes photons due to cavity decay (absorption, scattering, reflection of anti-Stokes photons in different directions without return to the RM), the fifth term represents all the anti - Stokes photons resulting from the spontaneous scattering in Raman medium. The terms of Equation (4) can be defined as the following, the first term is the optical pumping photons that causes the PID in AM, the second and the third terms represent the decrease in the PID due to the spontaneous and the stimulated emission in AM respectively.

The terms of Equation (5) can be defined as the following, the first, second, and the third terms represent the decrease in ions population of the ground level of SA due to the absorption activity of this level, while the fourth term refers to the increase in the ions population in ground level due to the decay of excited level of SA. The terms of Equation (6) can be defined as the following, the first, second, and the third terms represent the addition in ions population of the ground level of SA due to decay of excited level, while the fourth term refers to the decrease in the ions population of excited level due to the decay of level.

The physical meaning of the equations parameters explained as the following: $\varnothing_L$ (cm^{-3})laser photons density, $K_g = \frac{2L_g\sigma_g}{\tau_{Rt}}(s^{-1})$ coupling coefficient $L_g(cm)$, is length of active medium, $\sigma_g(cm^2)$ is the emission cross section of active medium, N_g (cm^{-3}) is the population inversion density, $\tau_{Rt} = \frac{2l_c}{c}$ (s) is the life time of photon in cavity$K_a = \frac{2L_a\sigma_{ag}}{\tau_{Rt}}$ (s^{-1}) , is coupling coefficient between the photons and saturable absorber material, l_c (cm) is cavity length, σ_{ag} (cm^2) the absorption cross section of ground level of SA, L_a is length of SA,N_{ag} is population of ground level in SA (cm^{-3}), $\beta = \frac{\sigma_{ae}}{\sigma_{ag}}$, $\sigma_{ae}(cm^2)$ is the absorption cross of excited level of SA, N_{ae} (cm^{-3}) is the population of excite level in SA, $N_{ag} + N_{ae} = n_i$, where

output coupler reflectivity at laser photon, $\tau_s = \frac{2L_C}{c[L - ln\sqrt{RR_s}]}$ is the round trip losses of Stokes photons of the cavity, R_s is output coupler reflectivity at Stokes photons, $\tau_{as} = \frac{2L_C}{c[L - ln\sqrt{RR_{as}}]}$ is the round trip losses of anti-Stokes photons in the cavity, R_{as} is output coupler reflectivity at anti-Stokes. It is worth noting, it is imperative to make some physical and mathematical approximation. The first and the second term in Equation (4) can be neglected due the release and emission of PQS pulse in very short time compared to the time influence of the factors R_p , γ_g [15,16], also the fourth term in the Equation (5), so the fourth and the fifth terms in Equation (6) can be neglected due to long time decay of excited level of SA (level 2) and due to very short lifetime of level 4[17]. At initial time of construction of PQS pulse, Equation (1) can approach to zero $\left(\frac{d\phi_L}{dt} \approx 0.\right)$,$N_{ae} \approx 0.$,$N_g \approx N_{go}$,$N_{ag} \approx n_i$, then it is possible to appreciate the initial population inversion density N_{go} as the following expression:

$$N_{g0} = \frac{k_a N_{ao} + (\frac{(2ghc\ l_R\,(v_s\varnothing_s + v_{as}\varnothing_{as})}{\tau_{RT}}) + \frac{1}{\tau_L}}{K_g} \tag{7}$$

As well as at the time becomes that PQS pulse at its peak, Equation (1) can approach to zero $\left(\frac{d\phi_L}{dt} \approx 0.\right)$,$N_{ag} \approx 0.$,$N_g \approx N_{th}$,$N_{ae} \approx n_i$, then it is possible to estimate the threshold population inversion density

$$N_{th} = \frac{\beta K_a N_{a0} + (\frac{(2ghc\ l_R\,(v_s\varnothing_s + v_{as}\varnothing_{as})}{\tau_{RT}}) + \frac{1}{\tau_L}}{k_g} \tag{8}$$

And after the pulse release, can estimate the pulse energy (E) as the following expression[18].

$$E = \frac{(N_{go} - N_{gf})}{N_{go}} \frac{(N_{go} - N_{gf})\,hv}{\gamma} \tag{9}$$

Where N_{gf} it represents the final value of population inversion density, can be determined from the results of the numerical solution of Equation (4), h Blanks constant, v is the frequency. The duration of pulse (τ)as well can be estimated after the pulse release (from numerical solution results of Equations (1), (2) and (3)). It represents the pulse width at half maximum (FWHM). The power calculated by the relation:

$$P = \frac{E}{\tau} \tag{10}$$

3 Results and Discussion

The set of rate Equations (1), (2), (3), (4), (5) and (6) solving numerically by Rung-Kutta- Fehelberg method, Table 1 show the input data [19–21] used in computation:

Table 1. Input data of computations

Parameter	Value	Parameter	Value
K_{sp}	$2\times10^{-10}s^{-1}$	σ_e	$6.5\times10^{-19}cm^2$
v_R	$925\ cm^{-1}$	σ_{ae}	$0.55\times10^{-18}cm^2$
G	8.4cm/GW	σ_{ag}	$2.5\times10^{-18}\ cm^2$

Figure 3 shows the behavior of three pulses generated in the different AM lengths (PQS, Stokes, and anti-Stokes pulses). It appears that the peak pulses are decreasing with increasing AM length. The study explains this as a decrease in the initial population inversion value, which led to a decrease in the laser photons released from AM. This result led to a decrease in the Stokes and anti-Stokes photon density. The pulses peak a little later in time when the AM length and the duration time increase for each pulse due to the increase in the rising time of pulses.

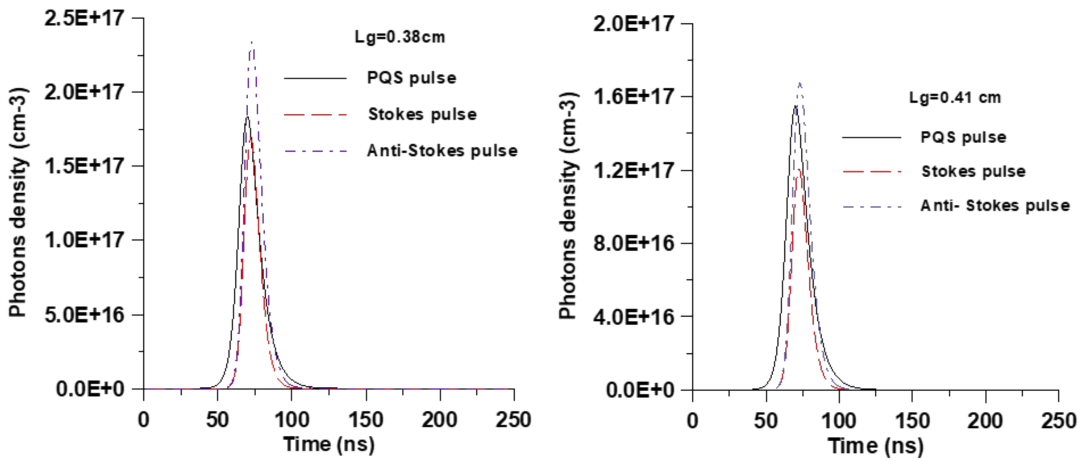

Fig 3. The profile PQS , Stokes , anti- Stokes pulses at L_g = 0.38 cm ,L_g= 0.41 cm

Figure 4 shows the profile of photon density and population inversion density (PID) for two values of AM length. The behavior shows a decrease in photon density and PID with an increase in AM length. This figure reinforces the results in Figure 3.

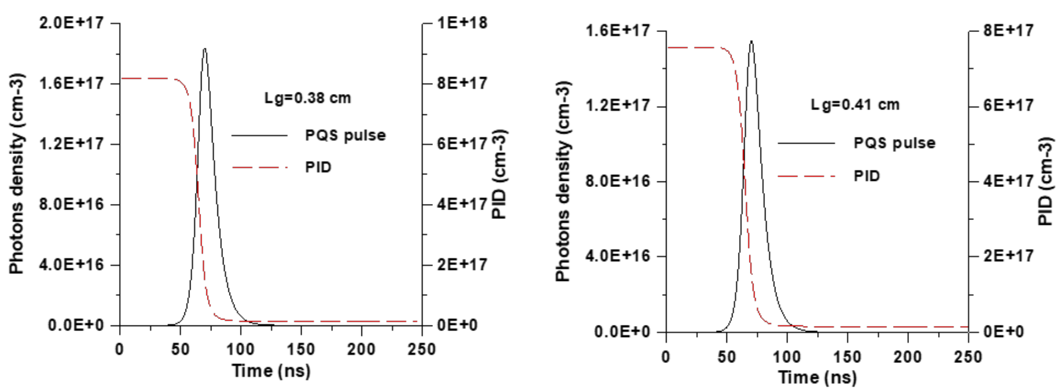

Fig 4. The profile of photons density, PID at L_g = 0.38 cm, L_g= 0.41 cm

Figure 5 shows the decrease in initial population inversion density (IPID) with an increase in the length of the AM. According to Equation (7), the increase in L_g leads to an increase in k_g, which thus leads to a decrease in the IPID and thus results in a decrease in threshold population inversion density (TIPD). The increase in the value of the final population inversion density (FPID) is shown by the increase in the length of the AM because of the remaining ions at the upper laser level and the unreleased energy. Also, there is the decrease in the value of the difference population inversion density (DPID) between the values of the IPID and FPID, a decrease due to the decrease in the initial value of the PID, and an increase in the FPID value due to the decrease in the TPID. Figure 6 shows the decrease in the maximum photon density (MPD) of the PQS pulse with an increase in the length of the AM due to the AM ions absorption of the PQS photons in the cavity. The result of the absorption led to a decrease in the IPID, as shown in Figure 5. The decrease in the MPD of Stokes and anti-Stokes is due to the continuous AM ion absorption; therefore, when the PQS photons fall on Raman medium, they will absorb and release the Stokes and anti-Stokes pulses, characterized by a decrease in their photon density values.

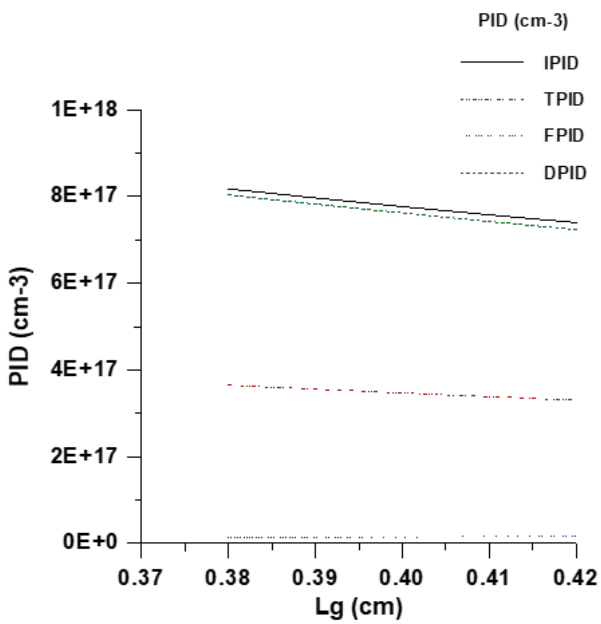

Fig 5. IPID, FPID, TPID, DPID as a function of Lg

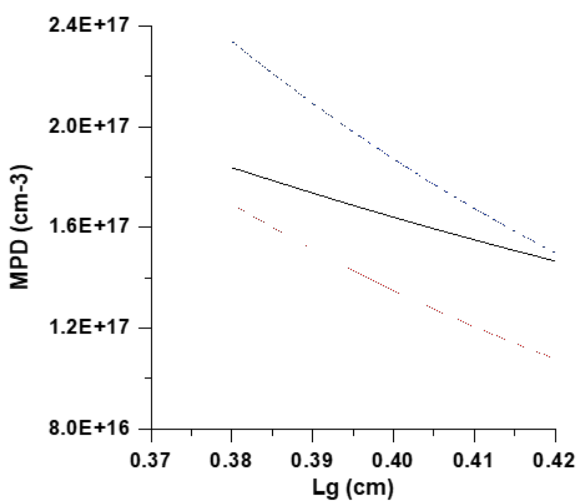

Fig 6. Maximum photons density of three pulses as a function of L_g

Figure 7 shows an increase in the duration of the three pulses generated (PQS, Stokes, and anti-Stokes) due to the increase in the rising time of the pulses. Figure 8 shows a decrease in the energy of PQS with an increase in the length of AM, due to the decrease in IPID as shown in Figure 5 and the decrease in the maximum photon density as shown in Figure 6.

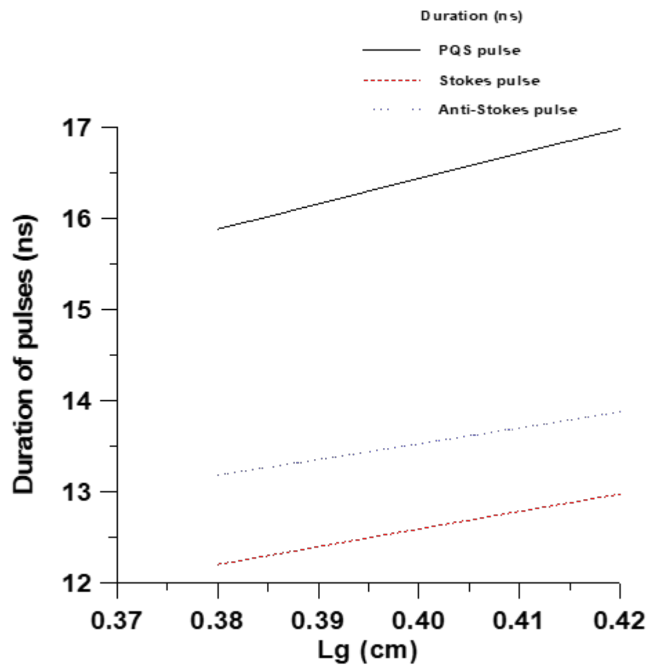

Fig 7. Duration pulse of three pulses generated as a function of L_g

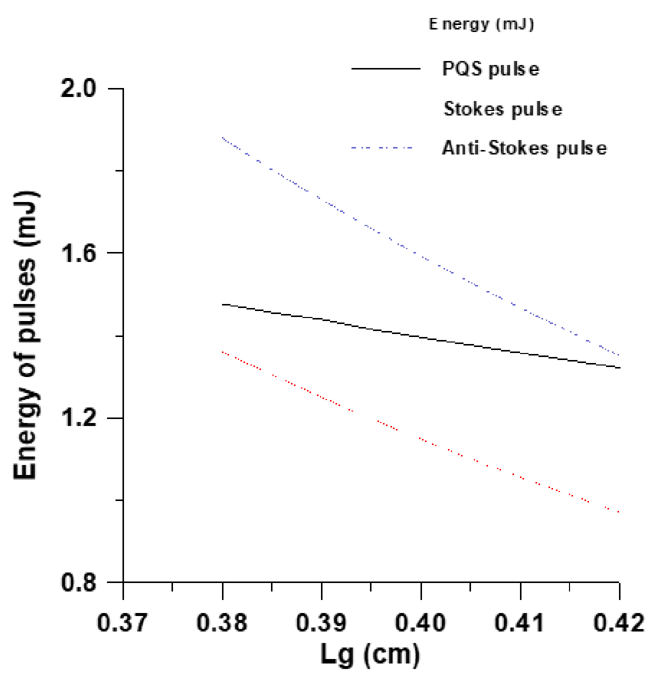

Fig 8. Energy of three pulses generated as a function of L_g

Figure 9 shows the power of PQS, Stokes, and anti-Stokes decrease with increasing AM length due to the increase in pulse duration as shown in Figure 7 and the decrease in energy as shown in Figure 8.

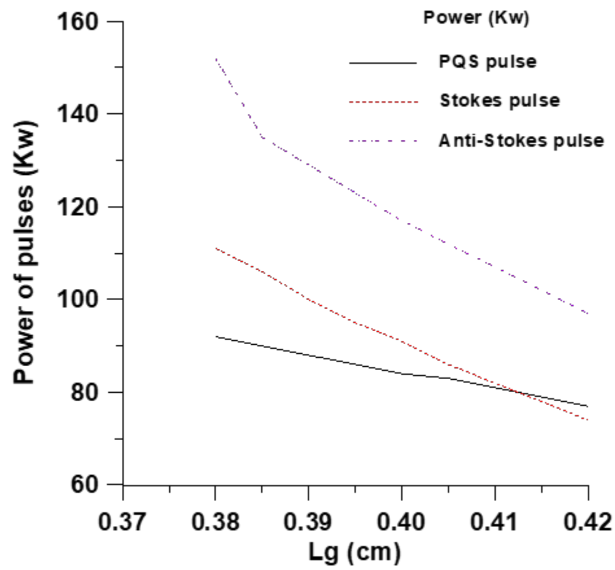

Fig 9. Power of three pulses generated as a function of Lg

4 Conclusion

The study concludes that the decreasing of the active medium length leads to emit high power pulses (passive Q-switching pulses, Stokes pulses, and anti-Stokes pulses) at advanced time (before 73 ns at Lg=0.38 cm, after 76 ns at Lg=0.41 cm as shown in Figures 1 and 2).

It is noticeable that the decreasing of the active medium length leads to increase in the energy of passive Q-switching pulses, Stokes pulses, and anti-Stokes pulses. So the decreasing of the active medium length leads to decrease in the pulses duration.

Thus, the shorter the length of the active medium in optical system which consists of passive Q-switch and Raman elements, can get high power of passive Q-switching pulses, Stokes pulses, and anti-Stokes pulses.

References

1) Hassan H, Salman AA, Munshid MA, Al-Janabi A. Passive Q-switching using Lead Sulfide suspension as a saturable absorber in 1.5 μm region. *Optical Fiber Technology*. 2019;52:101969. Available from: https://doi.org/10.1016/j.yofte.2019.101969.
2) Jiang Y, Nie M, Guo R, Fu X, Liu Q. Pushing the limit of pulse duration in Q-switched solid-state lasers with high gain. *Optics & Laser Technology*. 2020;129:106276. Available from: https://doi.org/10.1016/j.optlastec.2020.106276.
3) Tang J, Bai Z, Zhang D, Qi Y, Ding J, Wang Y, et al. Advances in All-Solid-State Passively Q-Switched Lasers Based on Cr4+:YAG Saturable Absorber. *Photonics*. 2021;8(4):1–14. Available from: https://doi.org/10.3390/photonics8040093.
4) Hu Y, Chu H, Li D, Li Y, Zhao S, Dong L, et al. Enhanced Q-switching performance of magnetite nanoparticle via compositional engineering with Ti3C2 MXene in the near infrared region. *Journal of Materials Science & Technology*. 2021;81:51–57. Available from: https://doi.org/10.1016/j.jmst.2020.11.064.
5) Ali Z, Abdulsada Z, Arasavalli N, Kadhim S, Akram H. Initial Transmission Influence on Saturable Absorber Absorption Activity of Passive Q-Switching Erbium -Doped Fiber Laser System. *University of Thi-Qar Journal of Science (UTJsci)*. 2023;10(2):224–229. Available from: https://doi.org/10.32792/utq/utjsci/v10i2.1139.
6) 6-Giese A, Körber M, Kostourou K, Kopf D, Kottcke M, Lohbreier J, et al. Passively Q-switched sub-100 ps Yb+3: YAG/Cr +4: YAG microchip laser: experimental results and numerical analysis. In: SPIE. -proceedings-of-spie on 23 Jul;vol. 12399. 2023;p. 187–197. Available from: https://doi.org/10.1117/12.2649057.
7) Marš M, Petkovšek R, Agrez V. Pump control based pulse on demand operation of frequency doubled Nd:YVO4. *Optics & Laser Technology*. 2022;152:1–6. Available from: https://doi.org/10.1016/j.optlastec.2022.108186.
8) Wu S, Yang M, Hao S, Ding C, Wang D. Trapezoidal Plane-Mirror Cavity for a Single Longitudinal Mode Nd:Yag Laser. *Optics Communications*. 2024;554. Available from: https://doi.org/10.1016/j.optcom.2023.130184.
9) Bai Y. Pumping wavelength related population inversion in Nd:doped laser. *AIP Advances*. 2020;10(10):1–6. Available from: https://doi.org/10.1063/5.0006436.
10) Zhou L, Fu H, Lv T, Wang C, Gao H, Li D, et al. Nonlinear Optical Characterization of 2D Materials. *Nanomaterials*. 2020;10(11):1–38. Available from: https://doi.org/10.3390/nano10112263.

11) Bodziony T, Kaczmarek SM. Structural Analysis of the BaWO4 Crystal Doped with Ce and Codoped with Na Ions Based on g-shift Parameters. *Crystals*. 2020;10(9):1–10. Available from: https://doi.org/10.3390/cryst10090789.
12) Ablett JM, Shieh SR, Balédent V, Woicik JC, Cockayne E, Shirley EL. X-ray spectroscopic and first-principles investigation of lead tungstate under pressure. *Physical Review B*. 2021;104(5). Available from: https://doi.org/10.1103/PhysRevB.104.054119.
13) Montalto L, Davì F, Dormenev V, Paone N, Rinaldi D. PbWO4 Acoustic Properties Measurement by Laser Ultrasonics with the Aim of Optical Damage Recovery. *Crystals*. 2023;13(4):1–17. Available from: https://doi.org/10.3390/cryst13040556.
14) Saad D, Hussein, Salih AM. Rate Equations Model to Simulate the Performance of Passive Q-Switched Laser with Raman Medium Optical System. *Indian Journal Of Science And Technology*. 2023;16(39):3353–3360. doi:10.17485/IJST/v16i39.1744.
15) Hussein ZA, Salih AKM. Investigation of Initial Transmission Effect on Saturable Absorber Optical Performance of Passive Q-Switching Doped Fiber Laser. *NeuroQuantology*. 2021;19(7):103–109. Available from: https://www.neuroquantology.com/media/article_pdfs/103-109_NtQBwGQ.pdf.
16) Hussein TM, Salih AKM. Simulation of Effective Beam Area Ratio Effect on Characteristics of Passive Q-Switched Fiber Doped Laser. *Journal of Optoelectronics Laser*. 2022;41(10):452–461. Available from: https://scholar.google.com/citations?view_op=view_citation&hl=en&user=L6Wtr44AAAAJ&citation_for_view=L6Wtr44AAAAJ:_Qo2XoVZTnwC.
17) Alonso VP, Weigand R, Snchez-Balmaseda M, Pérez JMG. Powerful algebraic model to design Q-switched lasers using saturable absorbers. *Optics and Laser Technology*. 2023;164:1–13. Available from: https://doi.org/10.1016/j.optlastec.2023.109506.
18) Hussein ZA, Salih AKM. Saturable absorber initial transmission effect on characteristics of passive Q-switching Er+3doped fiber laser. In: 3RD INTERNATIONAL SCIENTIFIC CONFERENCE OF ALKAFEEL UNIVERSITY (ISCKU 2021);vol. 2386, Issue 1 of AIP Conference Proceedimgs. 2022. Available from: https://doi.org/10.1063/5.0067126.
19) Chen W, Inagawa Y, Omatsu T, Tateda M, Takeuchi N, Usuki Y. Diode-pumped, self-stimulating, passively Q-switched Nd3+:PbWO4 Raman laser. *Optics Communications*. 2001;194(4-6):401–407. Available from: https://doi.org/10.1016/S0030-4018(01)01148-8.
20) Chen M, Dai S, Yin H, Zhu S, Li Z, Chen Z. Passively Q-switched yellow laser at 589 nm by intracavity frequency-doubled c-cut composite Nd: YVO4 self-Raman laser. *Optics & Laser Technology*. 2021;133. Available from: https://doi.org/10.1016/j.optlastec.2020.106534.
21) Lan R, Zhang F, Wang Z, Xiong W, Yuan H, Feng T. Efficient near-infrared, multiwavelengths PbWO4 Raman laser. *Optical Engineering*. 2017;56(9). Available from: https://doi.org/10.1117/1.OE.56.9.096112.